CHAPTER IV

RESULTS AND DISCUSSION

4.1 Characterization of the TS-1 Catalysts

4.1.1 XRD Results

XRD patterns of as-synthesized TS-1, with Si/Ti ratio in gel of 40, prepared by using different types of template are shown in Figure 4.1. The XRD patterns exhibit the characteristic reflection peaks of MFI structure. No other diffraction peaks for contaminating zeolite and for non-zeolite phases were detected. The intensities of three reflection peaks at 2θ of 8.7°, 23.2° and 45° in the XRD pattern of the zeolite product formed by pure TPABr are much higher than those in others. This is resulted from the effect of preferred orientation of crystal arrangement due to large crystals as indicated by the images of SEM. When a mixture of TPABr and TPAOH, 1:1 mole ratio, was used as a mixed template, the XRD pattern is very close to that prepared with pure TPAOH. After calcination the MFI structure of each sample was remained with increasing peak intensity, resulting from the removal of organic template from the zeolite pores.

4.1.2 SEM Images

SEM images of as-synthesized TS-1 prepared by using different types of template shown in Figure 4.2. The particle size and morphology are affected by the type of template. TS-1 synthesized by using TPAOH as template is cubic in particle shape with a size of about 270 nm, while TS-1 synthesized by using TPABr as template has a large prism shape. The particle size increases when the amount of TPABr increases. The SEM result could describe that using the mixed template, the particles had similar shape and only slightly bigger size comparing to those when pure TPAOH was used. Anyway, the particle sizes become very large when pure TPABr

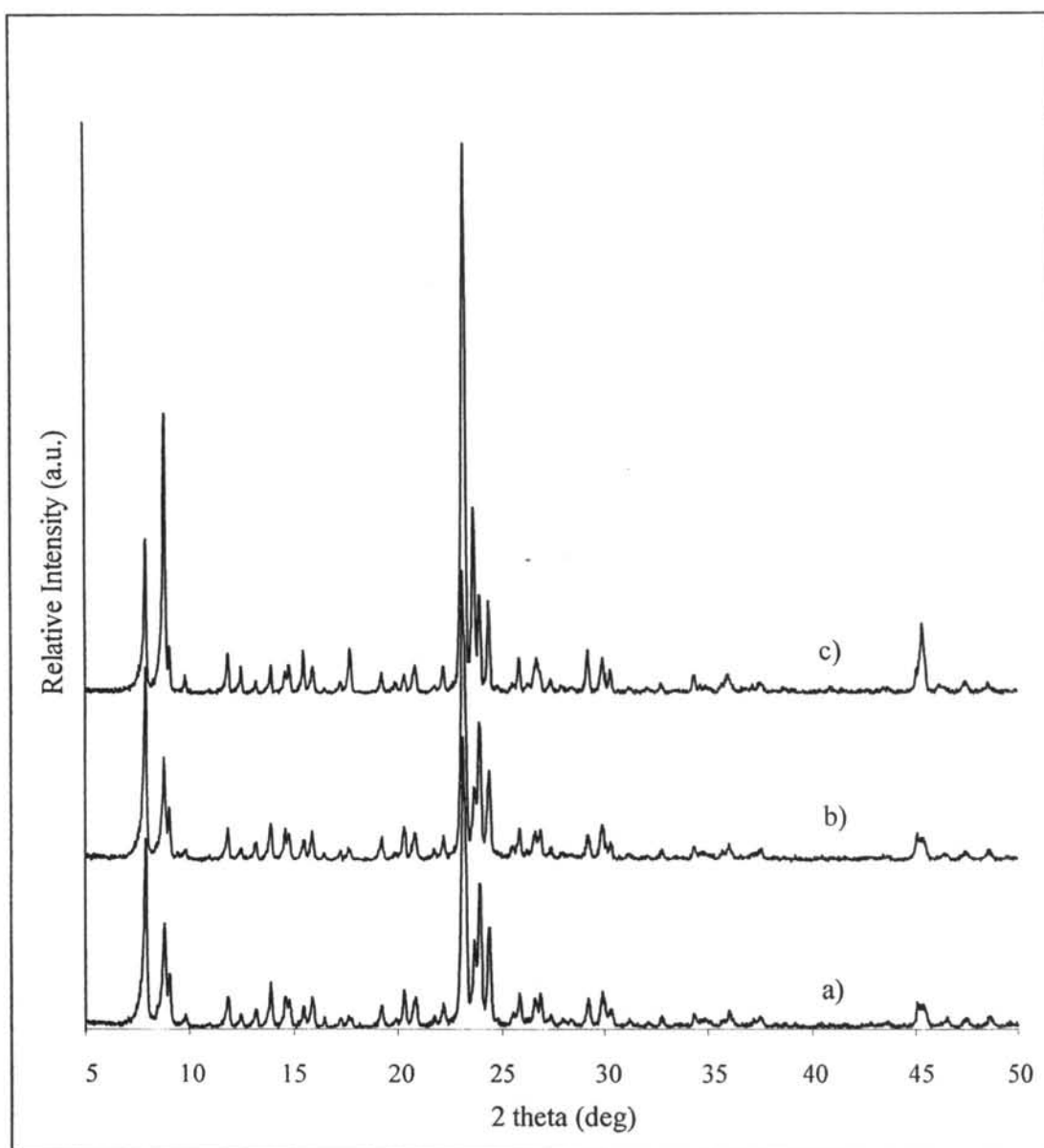was used as template. Table 4.1 shows the relation of the particle size and morphology of TS-1 catalyst.

Figure 4.1   XRD patterns of as-synthesized TS-1, with the Si/Ti ratio in gel of 40, prepared by using different templates, (a) pure TPAOH, (b) Mixed TPAOH and TPABr, (c) pure TPABr
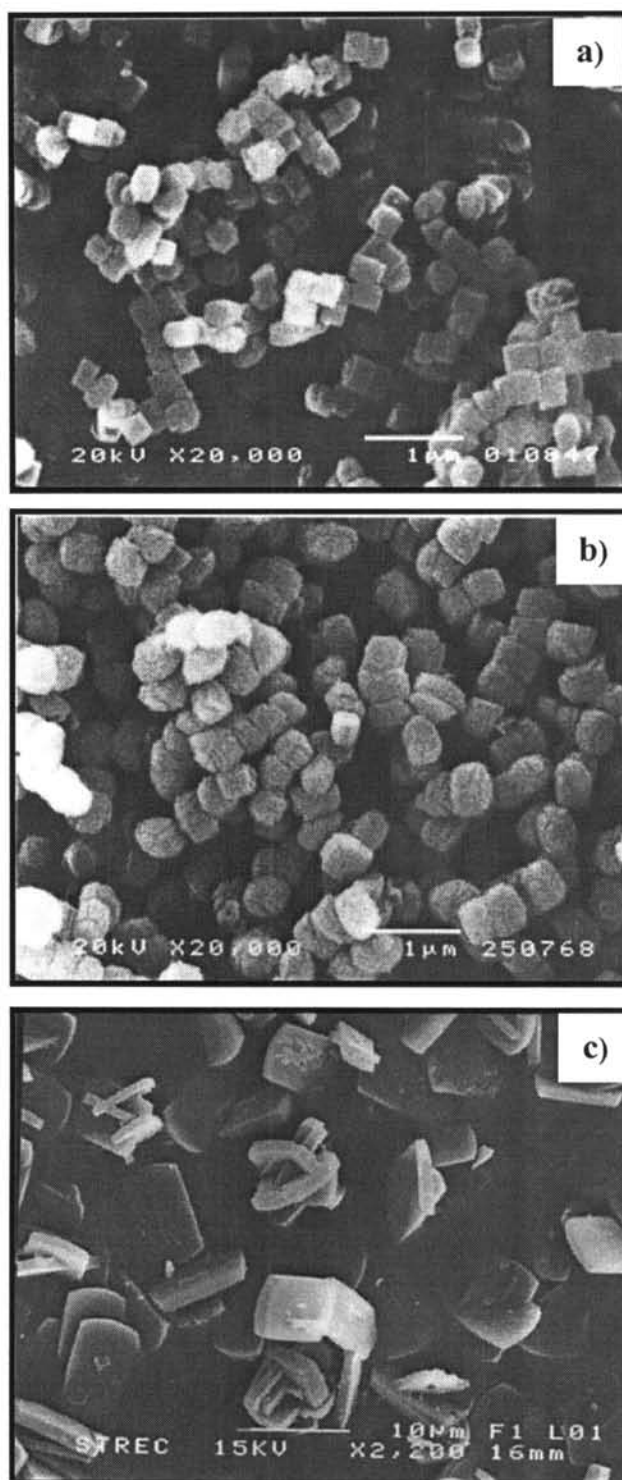
Figure 4.2 SEM images of as-synthesized TS-1 prepared by using different templates, a) pure TPAOH, b) mixed TPAOH and TPABr, c) pure TPABr

Table 4.1 The relation of template of gel on the mean particle size and morphology of as-synthesized TS-1 with the Si/Ti ratio in gel of 40

Templates	Mean particle size^a (nm)	Morphology
Pure TPAOH	270	Cubic
Mixed TPAOH and TPABr	330	Cubic-like
Pure TPABr	5000 x 8600 x 850^b	Tetragonal (sliced bread)

^{a} estimated from SEM images.

^{b} estimated in width x length x depth.

4.1.3 DR-UV

DR-UV spectra of the as-synthesized TS-1 samples are shown in Figure 4.3. The spectra of TS-1 samples prepared by using pure TPAOH and mixed templates are similar and exhibit a strong band 215 nm with a very weak shoulder band at 260 nm. The first band is attributed to the charge transfer from oxygen atom to Ti^{4+}. This is a characteristic band of tetrahedrally coordinated titanium in the solid framework and is generally observed for Ti-substituted molecular sieves [53]. The shoulder band indicates the presence of a small amount of extraframework Ti species [6]. In contrast, TS-1 prepared by using pure TPABr shows a continuum of UV absorption between 200 and 310 nm indicates the presence of a large amount of extraframework titanium species. TPABr is not good because it allows the formation of extraframework titanium species. The band at 215 nm of the sample prepared by using mixed templates incredibly increases in intensity compared to that observed for other samples and the shoulder near 270 nm is hardly observed. Among these different templates the mixed template of TPAOH and TPABr provides the highest opportunity for titanium to locate at the tetrahedrally coordinating framework position of the MFI structure without formation of extraframework titanium species. In addition using the mixed template can reduce the investment cost due to reduction the amount of expensive TPAOH as template in the preparation of TS-1.
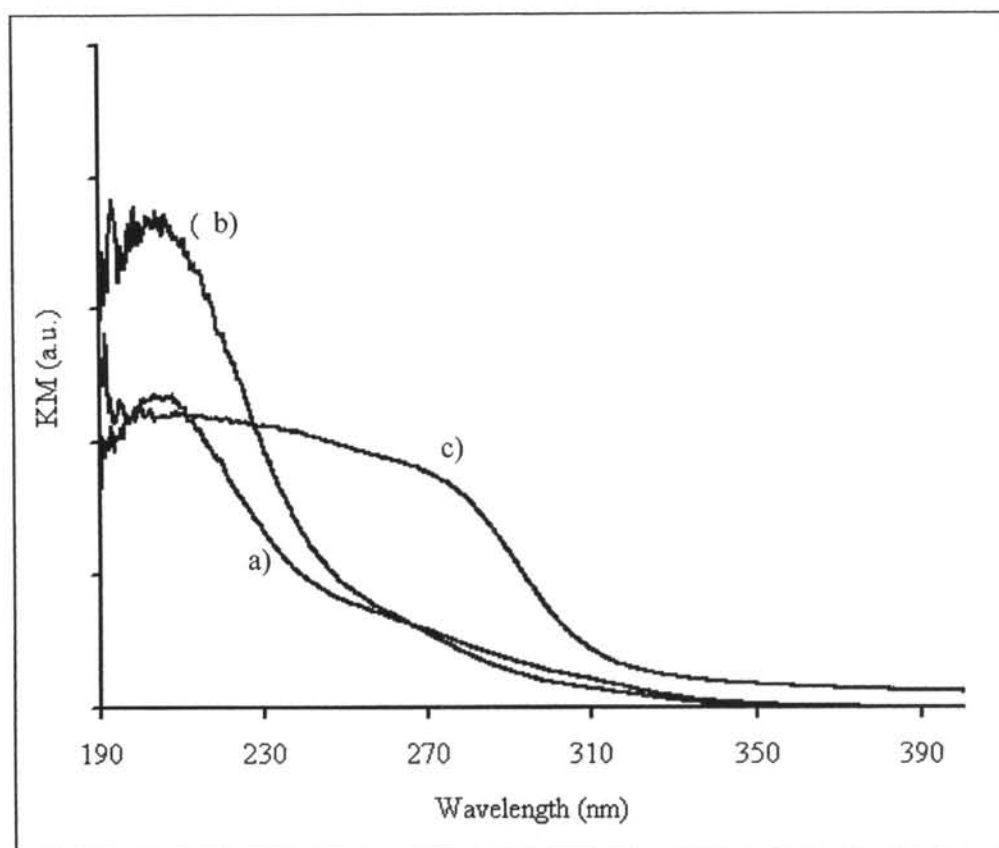
Figure 4.3 DR-UV spectra of as-synthesized TS-1 prepared by using different templates, (a) pure TPAOH, (b) mixed TPAOH and TPABr, (c) pure TPABr.

4.1.4 Si/Ti Ratios in Catalyst and Specific Surface Area of TS-1

The values of Si/Ti ratios and BET specific surface area of TS-1 catalysts are shown in Table 4.2. The Si/Ti ratios in catalyst analyzed are roughly near the ratios in gel or in the reactant mixture. The values of Si/Ti ratios increases in the order of using TPAOH > TPABr > mixed templates. However, the difference is not significant. All types of surface areas depend on the types of template. Although the BET specific surface areas of TS-1 seems not different, but the trend can indicate the slight decrease in the order of using mixed templates > TPAOH > TPABr. This is the same trend of external surface area. The particle size does not have a significant effect on the BET specific surface area. The surface roughness, as seen by SEM in Figure 4.2, of TS-1 particles increases in the same order as that of the BET surface area. This is confirmed by the same trend of the external surface area the difference of which is more obviously seen. The Langmuir specific surface area which is different order

from the BET data, is in the order of the samples of TPAOH ≅ mixed template >TPABr. This can be explained exactly by the particle size. The smaller the particle size, the larger the Langmuir specific surface area is.

Table 4.2   Values of Si/Ti ratios and specific surface area in TS-1 catalysts

Templates	Pure TPAOH	Mixed TPAOH+TPABr	Pure TPABr
Si/Ti in gel	40	40	40
Si/Ti in catalyst	42.0	45.8	44.3
BET specific surface area (m^2/g)	403	415	407
Langmuir specific surface area (m^2/g)	583	577	525
External surface area from t-plot (m^2/g)	18.7	13.4	3.77

4.2   Characterization of the Ti-MWW Samples

4.2.1   XRD Results of As-synthesized Ti-MWW Samples

The samples of Ti-MWW were synthesized by two different methods, Method I with two step crystallization and Method II with one step of crystallization. The crystallization time was varied in both methods. The XRD patterns of the as-synthesized samples are shown in Figure 4.4. All samples show characteristics peaks of MWW structure between the 2θ ranged from 5° to 30° with different peak intensity, *i.e.* crystallinity. The XRD patterns are totally consistent with that of the lamellar precursor of MWW topology, generally denoted as zeolite MCM-22 [54]. The 001 and 002 peaks at $2\theta = 3$-7° are characteristic of a layered structure along the *c*-direction. Other peaks are related with the crystalline sheets parallel to the *ab* planes. Method I gave the samples with higher intensity than Method II for the same crystallization time. Increasing crystallization time from 7 to 8 days results in the

increase in crystallinity of the samples prepared by Method I (Figure 4.4a-b) but the crystallinity does not increase further after 8 days. It should be pointed out herewith that the XRD peak at 2θ of $2.7°$ is due to the contamination of boron species. The crystallization time of 8 and 9 days provide some amount of boron species contaminated on the highly crystalline MWW structure. For the samples prepared by Method II, increasing crystallization time from 7-9 days cannot increase the crystallinity of Ti-MWW (Figure 4.4e-g).

4.2.2   SEM Images of As-synthesized Ti-MWW Samples

Figure 4.5 shows SEM images of Ti-MWW samples prepared by Method I with different crystallization time. All as-synthesized samples look like needle in shape but were actually thin platelets which grow aggregates by turning the light color edge toward outside. However, a few platelets turning the dark color front side can be observed in all images. The average size of the particles was 200-500 nm in length and 100 nm in thickness. For Ti-MWW crystallization, there was some amorphous phase left after crystallization for 7 and 8 days but the amorphous phase was completely transformed to crystalline phase after crystallization for 9 days. The result indicates that Ti-MWW crystallization was completed in 9 days. Combing XRD and SEM results, Method I with crystallization time of 9 days was chosen to be the appropriate condition for the synthesis of the Ti-MWW samples for further study in this work.
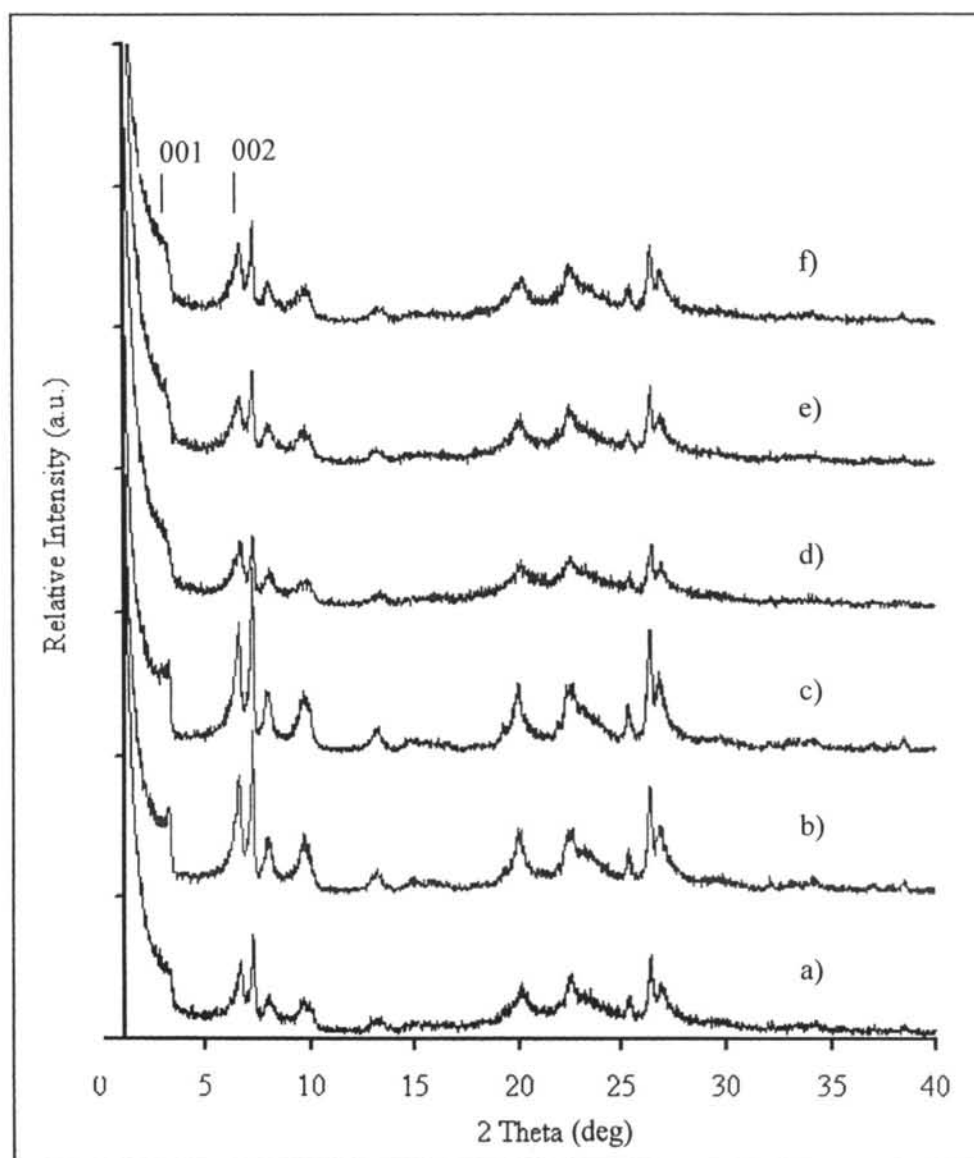
Figure 4.4 XRD patterns of as-synthesized Ti-MWW prepared by Method I with different crystallization time, a) 7 days, b) 8 days, and c) 9 days, and Method II with different crystallization time, d) 7 days, e) 8 days, and f) 9 days.
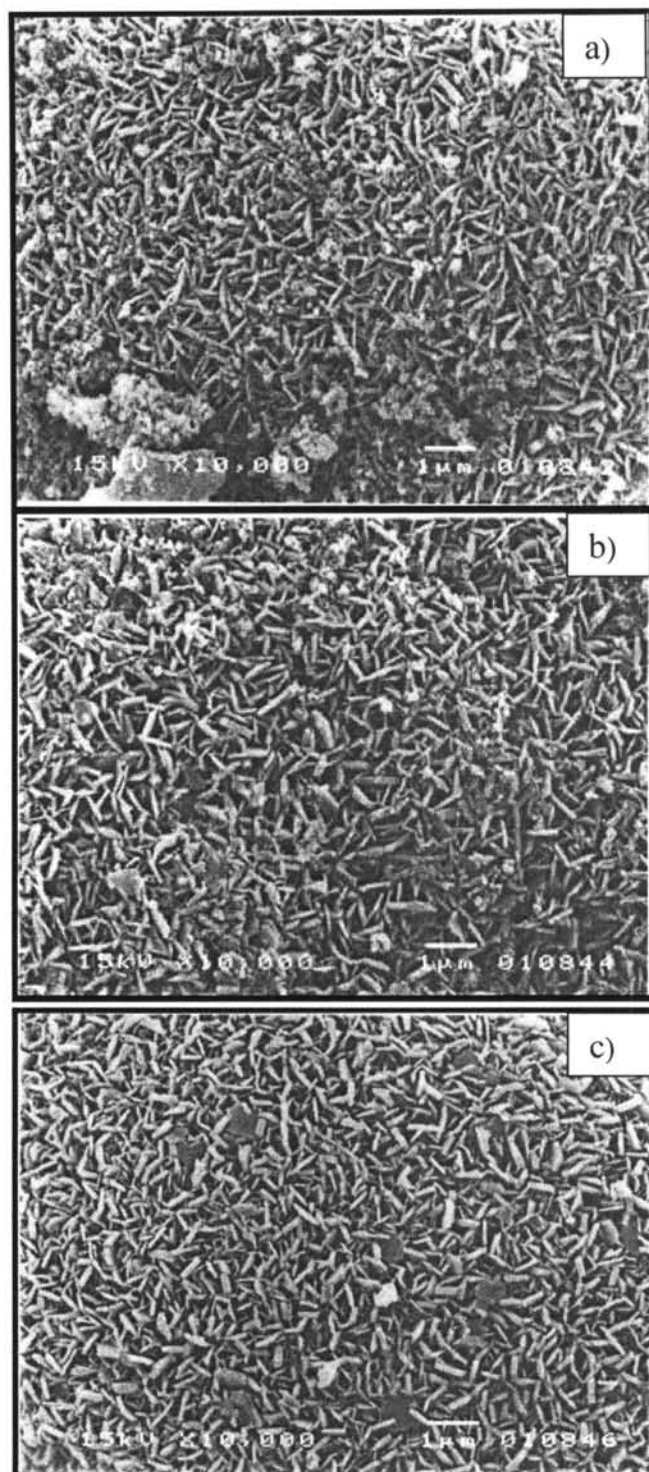
Figure 4.5 SEM images of as-synthesized Ti-MWW prepared by Method I with different crystallization time, a) 7 days, b) 8 days, and c) 9 days.

4.2.3 DR-UV of As-synthesized Ti-MWW Samples

The DR-UV spectra of as-synthesized Ti-MWW samples prepared by Method I with different crystallization time were shown in Figure 4.6. The spectra exhibit an intense band at 260 nm of octahedrally coordinated Ti and a shoulder band around 215 nm of framework tetrahedrally coordinated Ti. A band around 330 nm was not observed, indicating that no anatase-phase of bulk TiO_2 was formed during sample crystallization.
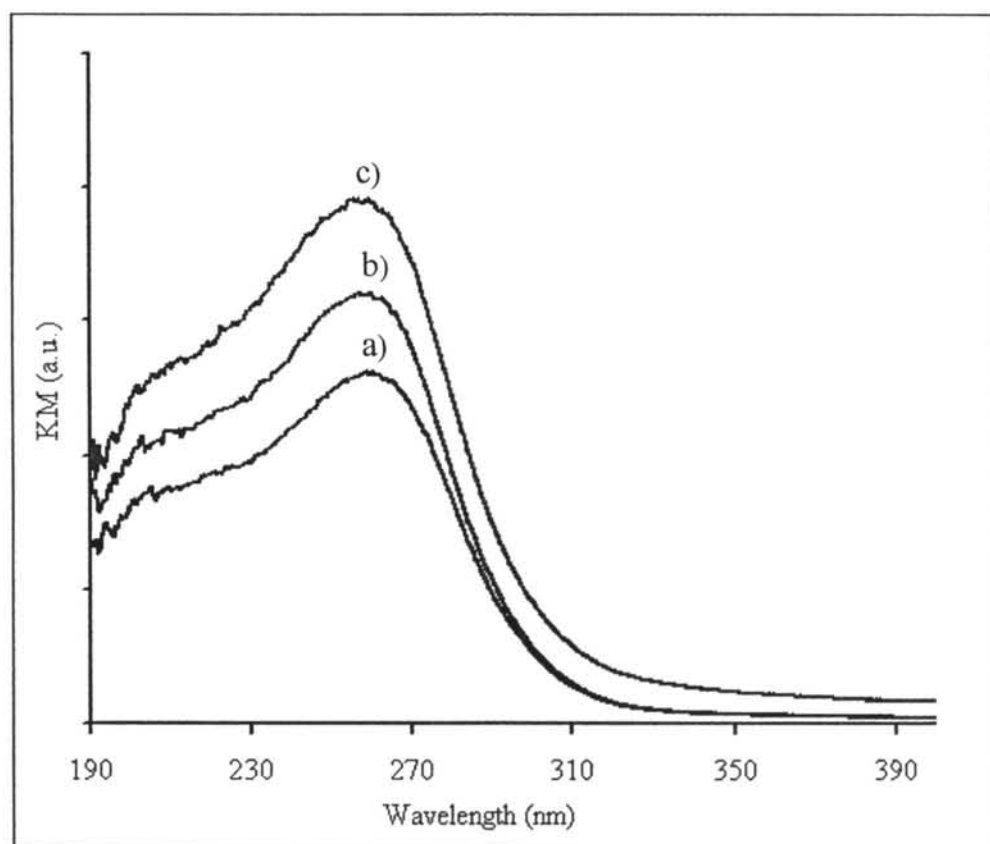

Figure 4.6 DR-UV spectra of as-synthesized Ti-MWW prepared by method I with different crystallization time, a) 7 days, b) 8 days, and c) 9 days.

4.2.4 XRD Results of Treated Ti-MWW Samples

Figure 4.7 shows XRD patterns of Ti-MWW samples treated under different conditions. Figure 4.7(a) is the XRD pattern of as-synthesized or untreated sample with lamellar structure of MWW. Figure 4.7(b) shows the decrease in intensity of 001 and 002 reflection peaks, which are a part of characteristic of lamellar MWW structure, as well as the decrease of other peaks at 2θ of 13.3° and 20° after acid treatment of the as-synthesized sample. After the calcination of the acid treated sample, the first two peaks were completely disappeared and a new peak at 2θ of 14.7° was noticed as shown in Figure 4.7(c). The new peak also found in the calcined sample without acid treatment. Therefore calcination results in the change from lamellar toward three-dimension structure by connection the layers next to each other or so-called reengineered. Without acid treatment the lamellar can be completely transformed to the three-dimension structure upon calcination. With acid treatment the structure transformation was not complete. The treatment of as-synthesized sample by calcination without acid treatment has well resolved XRD pattern as shown in Figure 4.7(d) which indicates the high ordered of three dimensional structure of MWW. One should not jump to the conclusion of choosing the calcination treatment without acid treatment. Other sample characterization such as SEM and especially DR-UV should be co-considered.
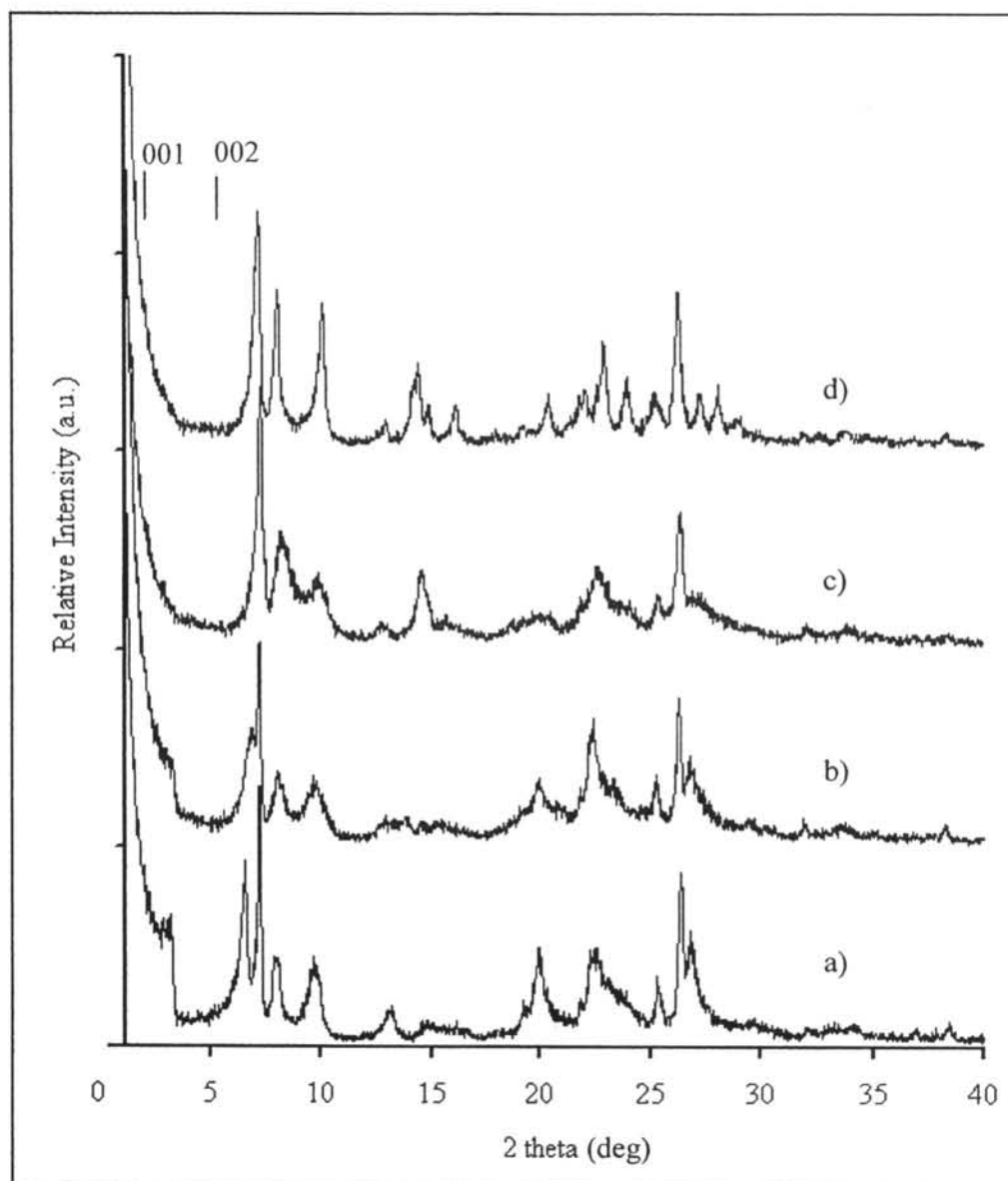
Figure 4.7 XRD patterns of Ti-MWW prepared by method I with crystallization time of 9 days, a) as-synthesized sample, b) acid treated sample without calcination, c) calcined sample after acid treatment, and d) calcined sample without acid treatment.

4.2.5 SEM Images of Treated Ti-MWW Samples

The SEM images the Ti-MWW samples calcined after acid treatment and calcined without acid treatment are shown in Figure 4.8. Comparing to SEM picture in Figure 4.5(c), the size of Ti-MWW particles is unchanged after calcination with or without acid treatment. The edge of the platelets is deformed to irregular form after acid treatment while unchanged after calcination without acid treatment. The platelets have more random orientation in the case of calcination without acid treatment than the as-synthesized sample and this is in agreed with the sharp and well resolved XRD peaks in Figure 4.7(d).
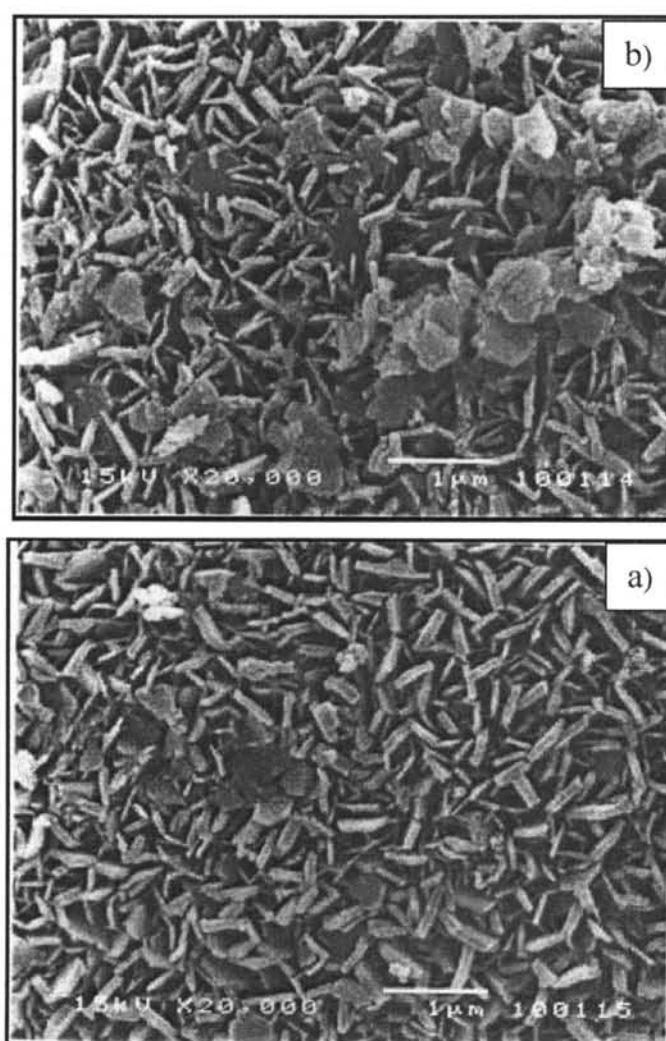

Figure 4.8   SEM images of Ti-MWW prepared by method I with crystallization time of 9 days, a) calcined after acid treatment, b) calcined without acid treatment.

4.2.6 DR-UV of Treated Ti-MWW Samples

Figure 4.9 shows the DR-UV spectra of Ti-MWW samples obtained by acid treatment before calcination Figure 4.9(a-c) and calcination without acid treatment Figure 4.9(d). It is obvious that acid treatment of Ti-MWW samples canabsolutely get rid off the extra-framework Ti species the band of which is located at 220 nm. The longer crystallization time provides slightly higher framework Ti species. The calcined sample without acid treatment has more unrequired non-framework Ti species including a tailing band at 310 nm which is assigned to bulk TiO_2. The results indicate that the removal of organic template by conventional calcination is not appropriate for Ti-MWW although the highest crystallinity can be obtained by calcination without acid treatment. DR-UV is the most criteria and beneficial among other methods of characterization.
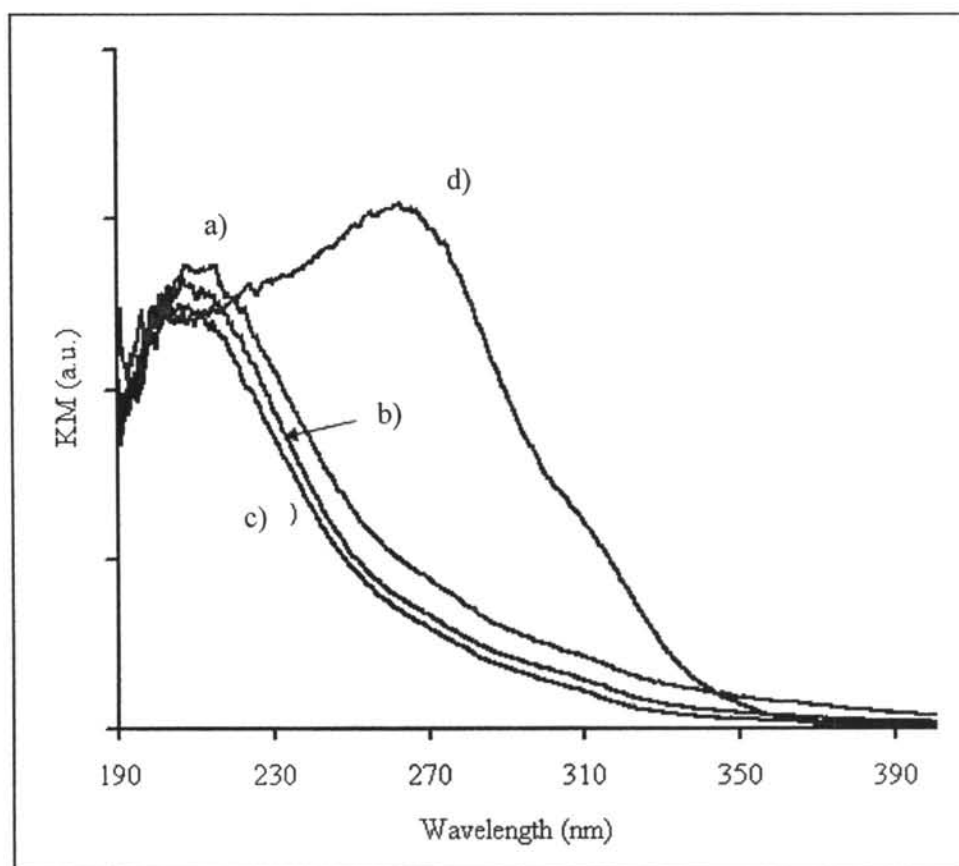

Figure 4.9   DR-UV spectra of Ti-MWW prepared by method I with different crystallization time, a) 7 days, b) 8 days, c) 9 days, followed by acid treatment before calcination, and d) 9 days, followed by calcination without acid treatment.

4.2.7 Compositions and Different Types of Surface Area of Ti-MWW

Compositions and different types of surface area of Ti-MWW prepared by method I with crystallization time of 9 days are shown in Table 4.3. The addition of Si, Ti and B in the gel mixture before crystallization did not completely incorporate in the structure. Acid treatment decreases the amount of Ti and B, increasing the ratio of Si/Ti and of Si/B, but increases the BET and Langmuir types of surface area of catalyst. However, the calcination without acid treatment provides the slightly larger external surface area of Ti-MWW comparing to the calcination after acid treatment. According to all results of characterization especially the DR-UV spectra of Ti-MWW, the catalyst prepared by Method I with crystallization time of 9 days and treated with 2N HNO_3 under reflux for 3 h, followed by calcination at 540 °C tends to be the most potential catalyst among the Ti-MWW samples prepared in this work. Both samples calcined after acid treatment and without acid treatment were chosen for the activity test in the catalysis of phenol hydroxylation in next section.

Table 4.3 Compositions and different types of surface area of Ti-MWW prepared by method I with crystallization time of 9 days

Properties	Gel mixture	Calcined Ti-MWW without acid treatment	Calcined Ti-MWW after acid treatment
Si/B ratio	0.75	21.46	31.22
Si/Ti ratio	40	36.23	77.46
BET specific surface area (m^2/g)	-	459	482
Langmuir specific surface area (m^2/g)	-	619	646
External surface area form t-plot $(m^2/g)^b$	-	89	77

4.3   Activity Test for Phenol Hydroxylation

4.3.1 Activity of Various Catalysts

Three calcined TS-1 samples prepared by using different types of template and two Ti-MWW samples calcined after acid treatment and calcined without acid treatment were chosen to test for the activity in the catalytic reaction of phenol hydroxylation. The hydroxylation of phenol by H_2O_2 is shown in Scheme 4.1. Hydroquinone is easily further oxidized by H_2O_2 to p-benzoquinone. Catechol is very difficulty oxidized by H_2O_2 to o-benzoquinone because it formed intramolecular hydrogen bonding. The notations of TS-1 samples are ended with a part of the template; for instance, TS-1-OH for TPAOH, TS-1-Br for TPABr, and TS-1-Mix for mixed TPAOH and TPABr. The Ti-MWW sample notation ended with –acid is for acid treatment before calcination and without ending is for calcination without acid treatment.   The results of the activity test of those five titanosilicate catalysts are shown in Table 4.4.
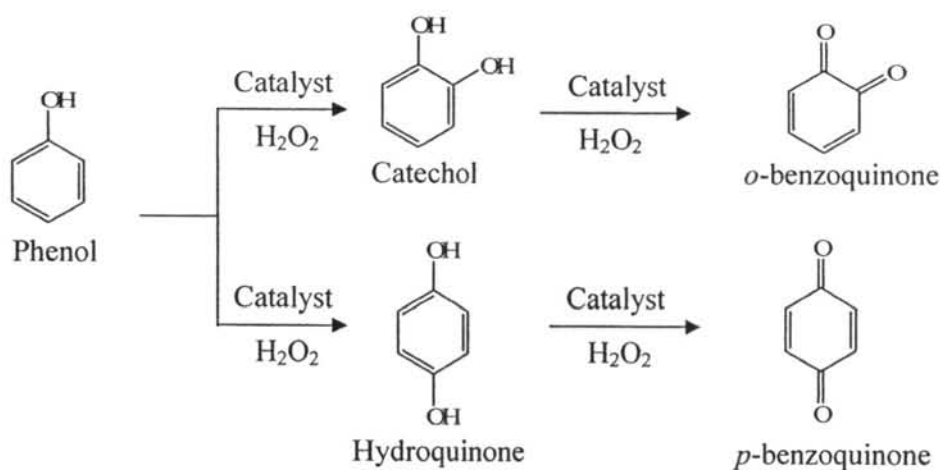
Scheme 4.1   The products of the hydroxylation of phenol.

Table 4.4   The activities of TS-1 and Ti-MWW catalysts in phenol hydroxylation[a] with H_2O_2 as oxidant

Calcined Catalysts	Conversion (mol %)	TON[b]	Total yield (mol %)	Product selectivity (mol%)			para/ortho[c] (molar ratio)
				HQ	p-BQ	CA	
TS-1-Br	25.0	38	6.9	6.4	74.4	19.2	4.2
TS-1-OH	30.9	85	18.9	9.5	61.3	29.2	2.4
TS-1-Mix	34.4	139	25	28.7	37.7	33.6	1.9
Ti-MWW	5.2	8	2.2	0.5	98.9	0.6	165.7
Ti-MWW-acid	8.1	26	2.8	0.8	96.5	2.7	36.0

[a] Reaction condition: 5 mmol phenol, 2.5 mmol H_2O_2 (30 wt.%), 50 mg catalyst, 5 g H_2O as solvent, temperature of 60°C and reaction time of 5 h.

[b] Turn over number as (HQ+p-BQ+CA) in mol/Ti in mol.

[c] (HQ+p-BQ)/CA.

All TS-1 samples are active in the phenol oxidation. The conversion of phenol and the total product yield increase in the order of TS-1-Mix > TS-1-OH > TS-1-Br. Within the group of TS-1 catalysts, the phenol conversion and product yield are not affected by the particle size alone. It is more obvious to explain result by the external surface area. The external surface area of the catalysts increases in the order of TS-1-Mix > TS-1-OH > TS-1-Br. The higher of the external surface area, the more the conversion of catalyst are.

It is obvious that all three TS-1 samples are much more active than Ti-MWW samples. The structure plays important role on the different activity. Ti-MWW-acid exhibits higher phenol conversion than Ti-MWW that is explained by both BET and Langmuir specific surface area, *i.e.* Ti-MWW-acid has larger surface area than Ti-MWW.

In general, the product yield is used in determination of the amount of product compared to the same amount of starting material. In heterogeneous systems, the use of TON or turn over number is very useful when the numbers of active species in the catalysts are not the same. The TON values in Table 4.4 are agreed with the conversion, *i.e.* TS-1-Mix > TS-1-OH > TS-1-Br > Ti-MWW-acid > Ti-MWW. The difference in TON is in the greater extent to the difference in phenol conversion. The

reason is that only titanium atoms in the tetrahedral framework site are active for this type of reaction. The enormous number of titanium atoms of TS-1-Br and Ti-MWW locate in the inactive non-framework site as confirmed by DR-UV spectra. To create and transfer nascent oxygen to phenol, H_2O_2 could bind to tetrahedral Ti due to available vacant coordination sites but octahedral Ti does not have a vacant site.

The Si/Ti ratios in catalyst are not the reason of low activity of Ti-MWW samples compared to TS-1 catalysts because the ratios are not related to the conversion and the TON values. Due to performing the catalytic reaction for the same period, TON in Table 4.4 can be directly used in evaluation of rate of reaction. The rates of phenol hydroxylation catalyzed by various catalysts are in the order of TS-1-Mix > TS-1-OH > TS-1-Br > Ti-MWW-acid > Ti-MWW.

The product selectivity is varied depending on the type of catalysts. The selectivity to p-benzoquinone decreases in the order of Ti-MWW > Ti-MWW-acid > TS-1-Br > TS-1-OH > TS-1-Mix. Interestingly, Ti-MWW provides the most selectivity to p-benzoquinone up to 98.9%. Ti-MWW-acid has slightly lower selectivity of to Ti-MWW, *i.e.* 96.5%. Considering the reaction catalyzed by TS-1, when the selectivity to p-benzoquinone decreases, that to catechol preferably increases and that to hydroquinone slightly increases. Obviously, Ti-MWW catalyst without acid treatment favors the production of p-benzoquinone only. When production of catechol is preferred, the very active TS-1-Mix can be used as catalyst and catechol can be separated, if wanted, in the highest yield.

At the higher H_2O_2 concentrations, more p-benzoquinone was polymeric oxidation to tar by consumption of H_2O_2. A higher ratio of phenol/H_2O_2 led to higher efficiency of H_2O_2 [13, 71].

4.3.2 Effect of Solvent Types

The activities of TS-1-Mix and Ti-MWW-acid catalysts in phenol hydroxylation performed in various solvents are shown in Table 4.5. Phenol is readily soluble in water but insoluble in a nonpolar solvent as dichloromethane. Changing from water to polar organic solvents like methanol, acetone and acetronitrile causes the drastic decrease of phenol conversion and TON values for both groups of catalysts. The highest activity in water media and the use of H_2O_2 as oxidant make the process economic and friendly to environment. For TS-1-Mix the selectivity to p-benzoquinone in organic solvents tremendously increases but not different among

themselves. Both catalytic formation of hydroquinone and catechol are more forbidden in the presence of polar organic solvents.

Table 4.5   The activities of TS-1-Mix and Ti-MWW-acid catalysts in phenol hydroxylation performed in various solvents[a]

Calcined Catalyst	Solvent	Conv. (mol%)	TON[b]	Product selectivity (mol%)			para/ortho[c] (molar ratio)
				HQ	p-BQ	CA	
TS-1-Mix	Water	34.4	139	28.7	37.7	33.6	1.97
	Methanol	2.5	2.4	2.3	84.7	13	6.7
	Acetone	2.4	2.5	1.8	86.9	11.4	7.8
	Acetonitrile	2.6	2.6	1.8	87.5	10.7	8.4
Ti-MWW- acid	Water	8.1	25.9	0.8	96.5	2.7	36.0
	Methanol	1.5	2.2	1.9	90.1	7.2	12.8
	Acetone	1.8	2.4	1.3	91.9	6.8	13.7
	Acetonitrile	1.7	2.4	1.3	93.1	5.6	16.7

[a] Reaction condition: 5 mmol phenol, 2.5 mmol H_2O_2 (30 wt.%), 50 mg catalyst, 5 g H_2O as solvent, temperature of 60°C, and reaction time of 5 h.

[b] Turn over number as (HQ+p-BQ+CA) in mol/Ti in mol.

[c] (HQ+p-BQ)/CA.

Table 4.6 show adsorption parameters for the adsorption of phenol from different polar solvents into TS-1 pores [69-70]. Henry's adsorption constant for water is very substantial compared to those for organic solvents resulting in the high activity coefficient of phenol to undergo a reaction such as the hydroxylation catalyzed by TS-1 in aqueous media. This can be ascribed to the strong adsorption of

phenol on the catalysts in this solvent, which is driven by the water-phenol solution. The activity coefficient of phenol calculated using UNIFAC software [69] is much higher in water than in the methanol and acetone (Table 4.6). Surprisingly, no adsorption phenomena were observed in methanol and acetone. With methanol or acetone as a solvent the concentration of phenol in the pores of TS-1 is about the same as seen from the Henry's constants.

Table 4.6 Henry's constants (K_p) for the adsorption of phenol from different solvents in small TS-1 crystals and activity coefficients (γ)

solvents	Henry's constant $(K_p)^a$	Activity coefficients $(\gamma)^b$
water	84.4	9.0535
methanol	0.7	0.5943
acetone	0.6	0.3047

[a] Determined by the Liquid-Phase Chromatographic Technique [70]

[b] Calculated with UNIFAC under reaction conditions (60°C) [69].

The low conversion in acetone can be explained by the formation of acetone peroxides and hydroperoxides [71] (Scheme 4.2), which is too bulky to react with titanium sites in the small pores of zeolites. This is supported by the fact that TS-1 is very poorly active for oxidation reactions when *tert*-butylhydroperoxide is used as an oxidant. The formation of those bulky compounds thus lowers the concentration of free hydrogen peroxide in the liquid phase and consequently in the pores of zeolites.
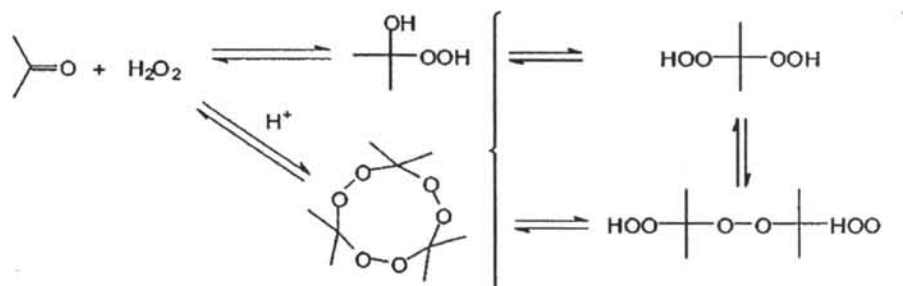
Scheme 4.2 Formation of alkylidene peroxides from acetone and hydrogen peroxide (14).

4.3.3 Effect of Reaction Time

The effect of reaction time for the activity and product selectivity over TS-Mix and Ti-MWW-acid are shown in Table 4.7. The extension of reaction time from 1 h to 5 h increases the activity in both of catalysts. For TS-1-Mix catalyst the selectivity to *p*-benzoquinone is strongly time dependent. The ratio of ortho to product increase would be higher if consider by para/ortho ratio. But for Ti-MWW-acid

catalyst, the time extending could increase the selectivity of p-BQ, but HQ and CA decrease. The increasing of Ti-MWW-acid quantity, it would more selective for para-product by consider on the increasing of para/ortho ratio.

Table 4.7 Catalytic activities and selectivity in phenol hydroxylation by H_2O_2 over TS-Mix and Ti-MWW-acid catalysts with various reaction time[a]

| Calcined Catalyst	Time (h.)	Conv. (mol%)	TON[b]	Product selectivity (mol%)			para/ortho[c] (molar ratio)
				HQ	p-BQ	CA	
TS-1-Mix	1	9	15.8	3.1	73	23.9	3.17
	3	27.5	107.7	26	44.6	29.4	2.4
	5	34.4	139	28.7	37.7	33.6	2
Ti-MWW-acid	1	2.3	4.2	1.2	93.5	5.3	17.9
	3	7.2	17.7	0.3	96.6	3.1	31.4
	5	8.1	25.9	0.8	96.5	2.7	36.0

[a] Reaction condition: 5 mmol phenol, 2.5 mmol H_2O_2 (30 wt.%), 50 mg catalyst, 5 g H_2O as solvent, temperature of 60°C.

[b] Turn over number as (HQ+p-BQ+CA) in mol/Ti in mol.

[c] (HQ+p-BQ)/CA.

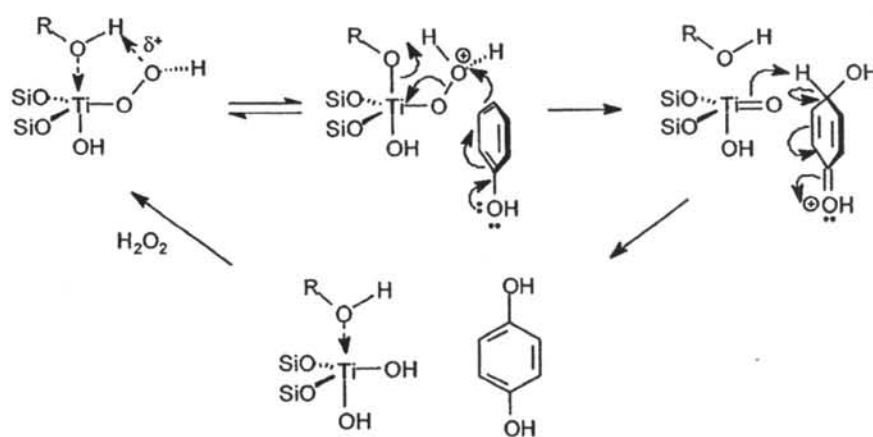### 4.3.4 Mechanism of Phenol Hydroxylation

To understand *para-* or *ortho-* hydroxylation, attention must be focused on the titanium sites. The interaction of protic solvents, such as alcohols and water, with Ti sites is well known and confirmed by spectroscopic studies. In literature, it is generally agreed that protic molecules coordinate to titanium, expanding its coordination sphere to 5 or 6. An increase in the average Ti–O bond length upon adsorption of methanol and water has been observed as well [23]. A five-membered ring with hydrogen bonds between methanol and the peroxo group at the titanium site has often been proposed as the active intermediate complex for TS-1 catalyzed reactions [9]. Scheme 4.3 shows possible configurations of the titanium active site with coordination of 1 or 2 protic solvent molecules (species (a), and (b)) and without solvent molecules (species (c)).
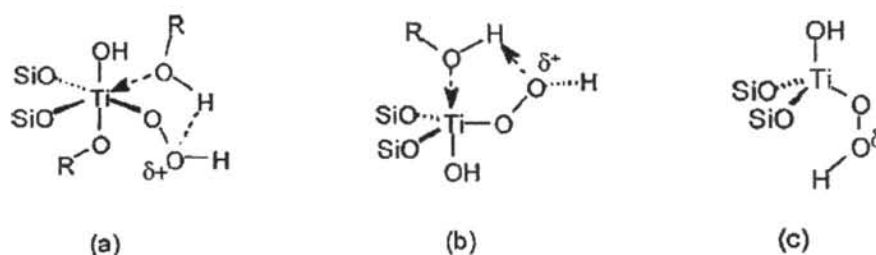
Scheme 4.3 Possible configurations of the hydroperoxo-titanium active site of TS-1: (a) hexacoordinate octahedral, (b) pentacoordinate trigonal bipyramidal, and (c) tetracoordinate tetrahedral.

The coordination of protic solvent molecules results in an increase in the size of the active titanium site. This narrows the catalysts channels, leading to a geometric constraint for an approaching phenol molecule. Hydrogen bonds of the phenolic OH with solvent OH groups will make the phenol molecule bulkier. Phenol, hydrogen-bonded to the solvent OH groups, will approach the bulky titanium site with the OH group pointing away from the titanium site (Scheme 4.4) yielding hydroquinone. Additionally, the presence of coordinated protic molecules close to the peroxo group could lead to hydrogen bond formation with the active site (species (a) and (b) in Scheme 4.3), destabilizing H-bonding with the phenol molecule assisting in *o*-hydroxylation (as shown in Schemes 4.5(a) and 4.5(b)).

On the other hand, in nonprotic solvents, phenol can take over the role of the protic solvent molecule. Although water is always present, its concentration in the hydrophobic TS-1 pores is expected to be low, as indicated by the extremely high K value of phenol in TS-1 with water as a solvent [23]. Thus, the existence of titanium sites without protic molecules coordinated is proposed (Scheme 4.3, species (c)). In that case another reaction pathway is opened, *i.e.*, the conversion via pentacoordinated (trigonal bipyramidal) Ti site, involving coordination of phenol to Ti peroxo species yielding catechol (Scheme 4.5(a)). This will be the case in aprotic solvents, such as acetone or acetonitrile. Protic solvents will compete with phenol, so that this pathway is not dominant in these solvents. Formation of catechol without coordination of phenol to the active titanium site takes place via a six-membered transition state involving phenol (see Scheme 4.5(b)).

Scheme 4.4 Proposed reaction mechanism for the formation of hydroquinone in phenol hydroxylation [23].
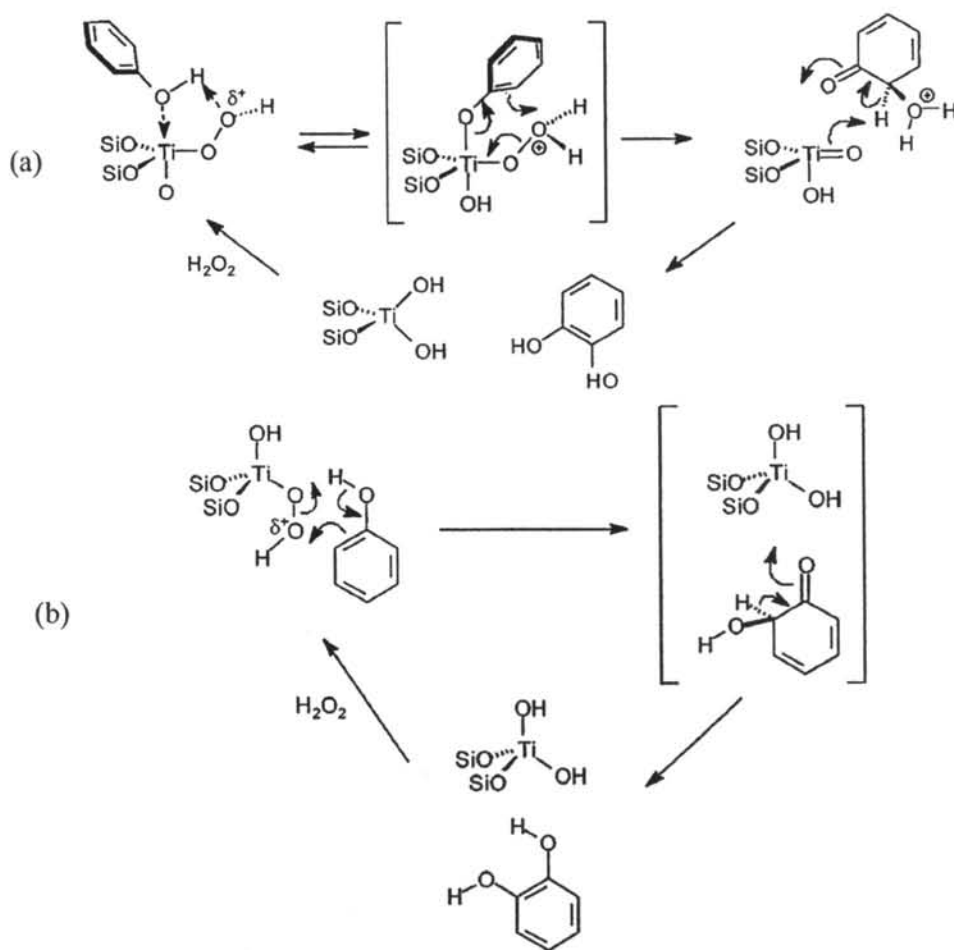
Scheme 4.5 Proposed reaction mechanism for the formation of catechol in phenol hydroxylation [23].